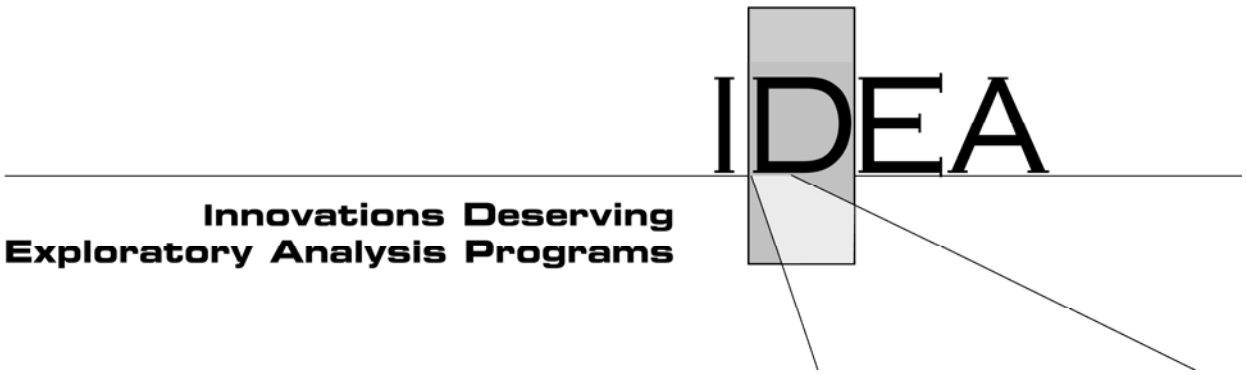

Highway IDEA Program

Novel Optical Fiber Sensors for Monitoring Bridge Structural Integrity

Final Report for Highway IDEA Project 124

Prepared by:
Maria Q. Feng, Newport Sensors, Inc.

March 2009

TRANSPORTATION RESEARCH BOARD
OF THE NATIONAL ACADEMIES

INNOVATIONS DESERVING EXPLORATORY ANALYSIS (IDEA) PROGRAMS
MANAGED BY THE TRANSPORTATION RESEARCH BOARD (TRB)

This NCHRP-IDEA investigation was completed as part of the National Cooperative Highway Research Program (NCHRP). The NCHRP-IDEA program is one of the four IDEA programs managed by the Transportation Research Board (TRB) to foster innovations in highway and intermodal surface transportation systems. The other three IDEA program areas are Transit-IDEA, which focuses on products and results for transit practice, in support of the Transit Cooperative Research Program (TCRP), Safety-IDEA, which focuses on motor carrier safety practice, in support of the Federal Motor Carrier Safety Administration and Federal Railroad Administration, and High Speed Rail-IDEA (HSR), which focuses on products and results for high speed rail practice, in support of the Federal Railroad Administration. The four IDEA program areas are integrated to promote the development and testing of nontraditional and innovative concepts, methods, and technologies for surface transportation systems.

For information on the IDEA Program contact IDEA Program, Transportation Research Board, 500 5th Street, N.W., Washington, D.C. 20001 (phone: 202/334-1461, fax: 202/334-3471, http://www.nationalacademies.org/trb/idea)

Novel Optical Fiber Sensors for Monitoring Bridge Structural Integrity

IDEA Program Final Report

For the period 1/8/2007 through 7/7/2008

NCHRP-124

Prepared for the IDEA Program

Transportation Research Board

National Research Council

By

Maria Q. Feng

Newport Sensors, Inc.

First Draft on 7/30/2008

Modified on 9/30/2008

Further Modified on 3/30/09

ACKNOWLEDGEMENT

This project is supported by the Innovations Deserving Exploratory Analysis (IDEA) Program, a part of the National Cooperative Highway Research Program (NCHRP), Transportation Research Board, the National Academies, and managed by Dr. Inam Jawed.

The project team would like to thank the NCHRP-IDEA Committee for their invaluable guidance and suggestions regarding the technical requirements for the proposed sensor system and constructive comments on this final report. The in-kind support provided by Caltrans for the field evaluation tests of the sensor system on two of the California highway bridges is also highly appreciated.

TABLE OF CONTENTS

EXECUTIVE SUMMARY

This IDEA project successfully developed a novel sensor system based on innovative integration of fiber optics and Moiré phenomena for measuring dynamic response of highway bridges to assess their structural integrity. The 18-month project was conducted in two phases. Work in the initial phase focused on the development of a prototype sensor system. Technical specifications of the proposed fiber optic accelerometer system were established, based on which a conceptual design of the system was developed. The sensor head consisted of a pair of parallel grating panels, a pendulum, and two pairs of fibers with collimators. Computer simulation was performed to determine optimal trade-off between the sensor's conflicting dynamic bandwidth and resolution, and furthermore the key design parameters including the optical grating pitch and the mass, stiffness, and damping of the pendulum. A special signal processing algorithm was developed to further broaden the dynamic bandwidth and enhance the measurement sensitivity of the accelerometer. An auto-inspection/auto-adjustment procedure was developed to achieve high accuracy and alignment in fabricating the sensor head. A portable prototype multi-channel accelerometer system was developed that included multiple sensor heads, a low-cost signal box (for sensor interrogation) and a PC (for signal processing).

In the second phase, the system was extensively tested in NSI, UCSD, and UNR laboratories under a variety of dynamic excitations including earthquake inputs on seismic shaking tables. Furthermore, the sensors were tested at two highway bridge sites in California under traffic excitations, in collaboration with Caltrans. These tests demonstrated superior performance of the new fiber optic acceleration system over its conventional electrical counterparts, including (1) total immunity to electromagnetic interference and lightning strikes, (2) unique safety in explosion-prone environments, (3) a small sensor head with a lightweight optical fiber cable facilitating convenient

installation on a long-span bridge, (4) robustness against environmental changes, and (5) much lower cost than most optical fiber sensors because of its simple signal processing.

The field test at one of the bridge sites was interviewed by and featured in the National Public Radio. Newport Sensors, Inc. has started to develop the fiber optic accelerometer system into commercial products. The availability of such a high-performance dynamic sensor system will promote the wide application of the emerging structural health monitoring technology for maintenance and management of highway bridges, as well as for real-time, remote post-event damage assessment and capacity estimation, based on the identification of change in structural dynamic characteristics from the measured structural vibration.

1. IDEA PRODUCT

This IDEA project developed an innovative sensing mechanism (the integration of fiber optics with Moiré phenomena) into a high-performance fiber optic dynamic sensor system for monitoring vibration of highway bridges under traffic, seismic, and other dynamic loads. The availability of such a high-performance dynamic sensor system will promote the wide application of the emerging structural health monitoring technology for maintenance and management of highway bridges, as well as for real-time, remote post-event damage assessment and capacity estimation, based on the identification of change in structural dynamic characteristics from the measured structural vibration.

The fiber optic dynamic sensor system developed in this project represents significant technological advancement and advantages over the currently available conventional counterparts (mainly electrical sensors), including (1) total immunity to electromagnetic interference and lightning strikes, (2) unique safety in explosion-prone environments, (3) a small sensor head with a lightweight optical fiber cable facilitating convenient installation on a long-span bridge, (4) robustness against environmental changes such as temperature and moisture, and (5) much lower cost than most optical fiber sensors because of its simple signal processing.

In addition to the establishment of a new knowledgebase regarding the innovative integration of fiber optics and Moiré phenomena, precision fabrication techniques, and sensor testing methods, this project delivered a prototype fiber optic accelerometer system consisting of multiple lightweight sensor heads, optical fiber cables a multi-channel control unit, together with a software package for operation control, power supply, sensor interrogation, data acquisition, signal processing, and display in real time.

2. CONCEPT AND INNOVATION

The novelty of the proposed technology lies in accurate measurement of displacement through innovative integration of fiber optics and Moiré phenomena. As shown in Figure 1, the fiber optic accelerometer contains a pairs of parallel optical grating panels, one fixed to the mass of the pendulum and the other to the sensor casing. The acceleration of the sensor casing (to be measured) is proportional to the relative displacement of the mass with respect to the casing when the dynamic properties of the pendulum system are appropriately designed.

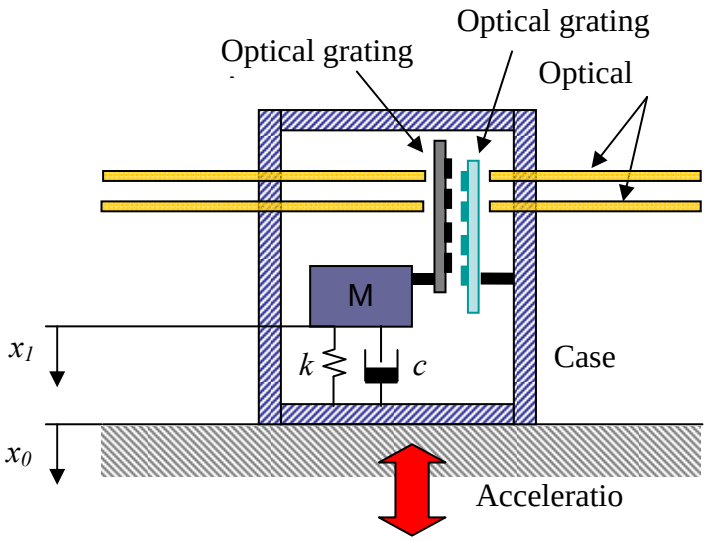

Figure 1. Conceptual Design of Moiré Fringe-Based Fiber Optic Accelerometer

Because one optical grating is fixed to the mass while the other is fixed to the sensor casing, the relative displacement of the two optical gratings is the same as the displacement between the mass and the sensor casing. When the two optical gratings

consisting of alternating parallel transparent and opaque strips (i.e. “rulings”) are overlaid, light will either be transmitted (when the transparent regions coincide) or be obstructed (when they do not coincide). If the rulings on one grating are aligned at a small angle relative to those on the other, then the loci of their intersections will be visible as dark moiré fringes running approximately perpendicular to the rulings as shown in Figure 2.

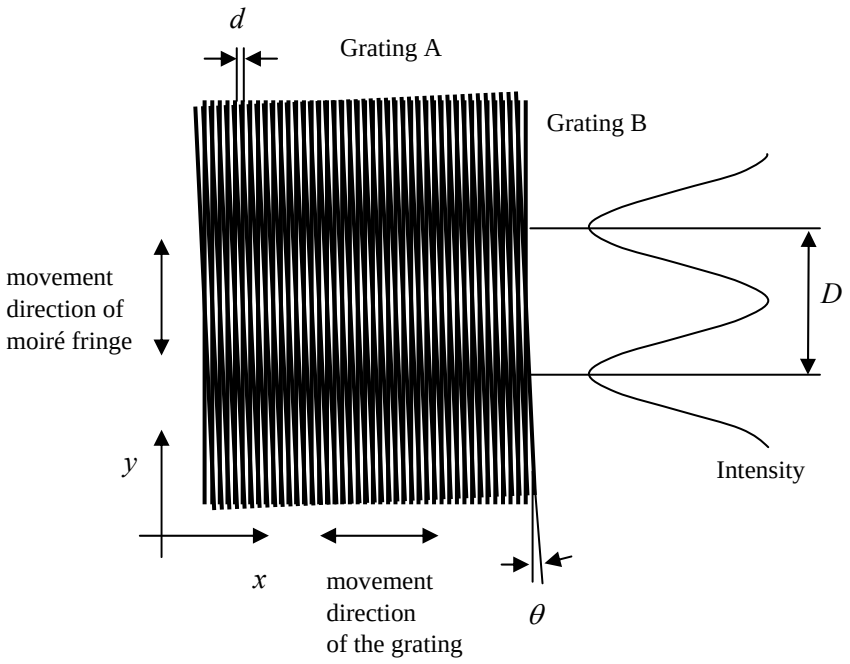

Figure 2. Moiré Fringes for Displacement Amplification

As the two parallel grating panels move with respect to each other in the *X* direction, the moiré fringes will move in the *Y* direction. The moiré fringes will shift by one pitch distance *D* in the *Y* direction when the two gratings shift in the *X* direction by one grating pitch *d*. The moiré fringe pitch *D* can be designed using the relation $D = d/\theta$ where θ is an angle subtended by the rulings of the two gratings. If one lets θ approach zero in the relation, the ratio *D*/*d* (i.e. the “displacement amplification”) can become very large. Consequently, if a small θ is chosen, one can considerably amplify a small grating

movement d into a large moiré fringe movement D. One would facilitate accurate displacement measurement by designing a small grating pitch, a small θ and thus a large D. The capability of measuring a small displacement with a high resolution is a significant advantage of this moiré fringe-based sensing mechanism.

The relative displacement between the two gratings can be measured by tracking the moiré fringes as they pass through one point. However, observing the moiré fringes at only one point yields no information regarding the direction of their movement, which is necessary to determine the direction of the relative movement of the two gratings. Fortunately, one can determine the direction as well as the amplitude of the displacement by tracking the fringes at two points which are separated by a quarter of the fringe width D across the fringe profile. In order to observe the moiré fringe at two different points, two pairs of optical fibers are placed perpendicular to the optical grating panels, as illustrated in Figure 1.

Furthermore, the displacement is translated into the acceleration of the mass through the dynamics of the pendulum. The pendulum is modeled as a single-degree-of-freedom dynamic system with a mass m, a spring stiffness k, and a damper c, as shown in Fig. 1. The equation of motion for the pendulum system is simply expressed as follows,

$$m\ddot{x} + c\dot{x} + kx = -m\ddot{x}_o \tag{1}$$

where $x=x_1-x_0$, the relative displacement between the pendulum mass and the sensor casing (i.e., the pendulum support) and the acceleration imparted to the sensor (i.e., the "excitation acceleration" in the right side of the Eq.) is to be measured.

Equation (1) can be rewritten in terms of the damping ratio ζ and the natural frequency of the pendulum ω_n:

$$\ddot{x} + 2\omega_n \zeta \dot{x} + \omega_n^2 x = -\ddot{x}_o \qquad (2)$$

where $\omega_n = \sqrt{\frac{k}{m}}$ and $\zeta = \frac{c}{2m\omega_n}$.

Assuming that $\ddot{x}_0 = A_{\text{excite}} e^{i\omega t}$, where ω is the frequency of the excitation acceleration, then the steady state response should be $x = D_{response} e^{i\omega t}$. In theory, the ratio of $D_{response}$ to A_{excite} should satisfy the following relation:

$$\frac{D_{response}}{A_{excite}} = \frac{-1}{\omega_n^2 - \omega^2 + 2i\omega_n \omega\zeta} \qquad (3)$$

Thus, if one sets $r = \frac{\omega}{\omega_n}$, then the deformation response factor, *R* can be expressed as follows:

$$R = \left| \frac{D_{response}}{A_{excite}} \right| \cdot \omega_n^2 = \frac{1}{\sqrt{\left(1 - r^2\right)^2 + \left(2r\zeta\right)^2}} \qquad (4)$$

where $r = \frac{\omega}{\omega_n}$. One can carefully design a system with a pendulum of mass *m* and spring stiffness *k* such that the natural frequency ω_n is much larger than ω. As ω_n increases, the ratio *r* approaches zero, and in turn the deformation response factor, *R* approaches unity. In this condition, Equation 4 demonstrates that the relative displacement, *x* is directly proportional to the excitation acceleration, $\ddot{x}_0$. Consequently, one can derive the acceleration of the sensor simply by gauging the relative displacement, *x* between the pendulum mass and the sensor casing. In other word,

$$x(t) = -\frac{R_d}{\omega_n^2} \ddot{x}_o\left(t - \frac{\phi}{\omega}\right) \qquad (5)$$

where ϕ is the phase lag between the actual and the measured accelerometers.

3. INVESTIGATION

3.1 PROPOSED RESEARCH OBJECTIVE AND PLAN

The overall objective of this IDEA project is to investigate whether it is feasible, from both technical and commercial points of view, to overcome technical difficulties and develop the proposed fiber optic accelerometer concept into a viable commercial product. The technical objectives include (1) conceptual design based on computer modeling and performance simulation, (2) development of high-precision and low-cost manufacturing/packaging processes and techniques that are crucial to the success, (3) development of algorithms and software for further enhancing the sensor sensitivity, (4) development of a cost-effective multiplexing and networking strategy, and (6) evaluation of technical feasibility through prototyping and testing.

Technical targets of the proof-of-concept prototypes to be developed in this project include high accuracy and sensitivity over a large bandwidth particularly in low frequencies, and low fabrication cost.

This IDEA project consists of two phases of study. The research tasks and milestones in the original proposals are as follows:

Phase I. Prototype Development (4 Quarters)

Tasks: (1) To develop conceptual design of the fiber optic sensor and perform simulation study of key technical parameters.
(2) To develop manufacturing/packing processes and techniques to achieve a high-precision and low-cost fabrications.
(3) To develop algorithms and a software package to further enhance the sensitivity of the sensor.
(4) To fabricate a prototype fiber optic sensor system.

Deliverable: A prototype fiber optic sensor system

Milestones: (1) Conceptual design by the end of the 2nd quarter.
(2) Prototype sensor system by the end of the 4th quarter.

Phase II. Feasibility Study (2 Quarters)

Tasks: (5) To evaluate technical feasibility through laboratory and field tests
(6) To evaluate cost and commercial feasibility.
Deliverable: A report documenting the testing data and feasibility evaluation.
Milestones: (1) Technical feasibility evaluation by the end of the 6th quarter
(2) Commercial feasibility evaluation by the end of the 6th quarter

The proposed project schedule is shown in Table 1.

Table 1. Project Schedule

Tasks	Phase	Q1	Q2	Q3	Q4	Q5	Q6
1. Conceptual Design & Simulation	I						
2. Manufacturing Processes/Techniques	I						
3. Software Development	I						
4. Proof-of-Concept Prototyping	I						
5. Technical Feasibility Evaluation	II						
6. Cost/Commercialization Evaluation	II						

3.2 INVESTIGATION APPROACHES AND RESULTS

All the proposed research tasks have been successfully carried out in this IDEA project. This section will describe the research approaches, processes, and results from conceptual design, computer software development, sensor system prototyping, to laboratory and field experimental evaluation, and finally the cost and commercial feasibility evaluation.

3.2.1 Conceptual Design

We first performed an extensive literature and market survey of the existing and emerging accelerometers suitable for monitoring bridge structures, based on which we determined the technical specifications of the proposed Moiré-fringe based fiber optic accelerometer. As shown in Table 2, the proposed specifications exceed the currently available accelerometers, particularly in terms of its resolution.

One of the advantage of the proposed fiber optic accelerometer is that the resolution is not limited by the measurement range, which make this sensor ideal for monitoring not only ambient vibration but also strong motion, both with a high resolution. Therefore, this sensor will be uniquely suited for vibration-based structural health monitoring purposes.

Table 2. Technical Specifications

Frequency Range	DC – 40Hz
Measuring Range	-3g – +3g
Resolution	$1.0X10^{-5}$ g

Based on the specification, we determined the values of key parameters of the sensor. Considering the sensing mechanism described in Chapter 2, the pendulum system inside the sensor head should be designed with a higher natural frequency in order to measure vibration of higher frequencies. However, the higher the natural frequency, the

stiffer the pendulum system and the smaller the relative displacement between the pair of grating panels. This in turn requires a smaller grating pitch in order to measure with a high resolution, which is technically challenging. For this purpose, computer simulation was performed to study an optimal trade-off between the conflicting dynamic bandwidth and resolution of the sensor. Based on the computer modeling and simulation results, the natural frequency of the pendulum is determined to be 80 Hz and the grating pitch 50 lines per mm.

Once we designed the grating panels, we were able to determine the distance between the pair of grating panels and then study light loss in relation to the distance. As a result, we determined that it is necessary to installed collimators at the end of the fibers in the sensor head.

3.2.2 Manufacturing Techniques

The sensing mechanism (as described in Fig.1) requires the pair of grating panels to be perfectly parallel and each pair of the optical fibers to be exactly aligned. Therefore, it is crucial to the success of this project to develop a high-precision and low-cost manufacturing/packaging process and techniques.

By consulting a precision sensor manufacturer, a member of the Advisory Board of this project, we designed and fabricated a special jig and an auto-inspection/auto-adjustment procedure that can assist accurate inspection and adjustment of the fiber installation and alignment. Photos in Figure 3 show the procedure of position adjustment using the fabricated jig.

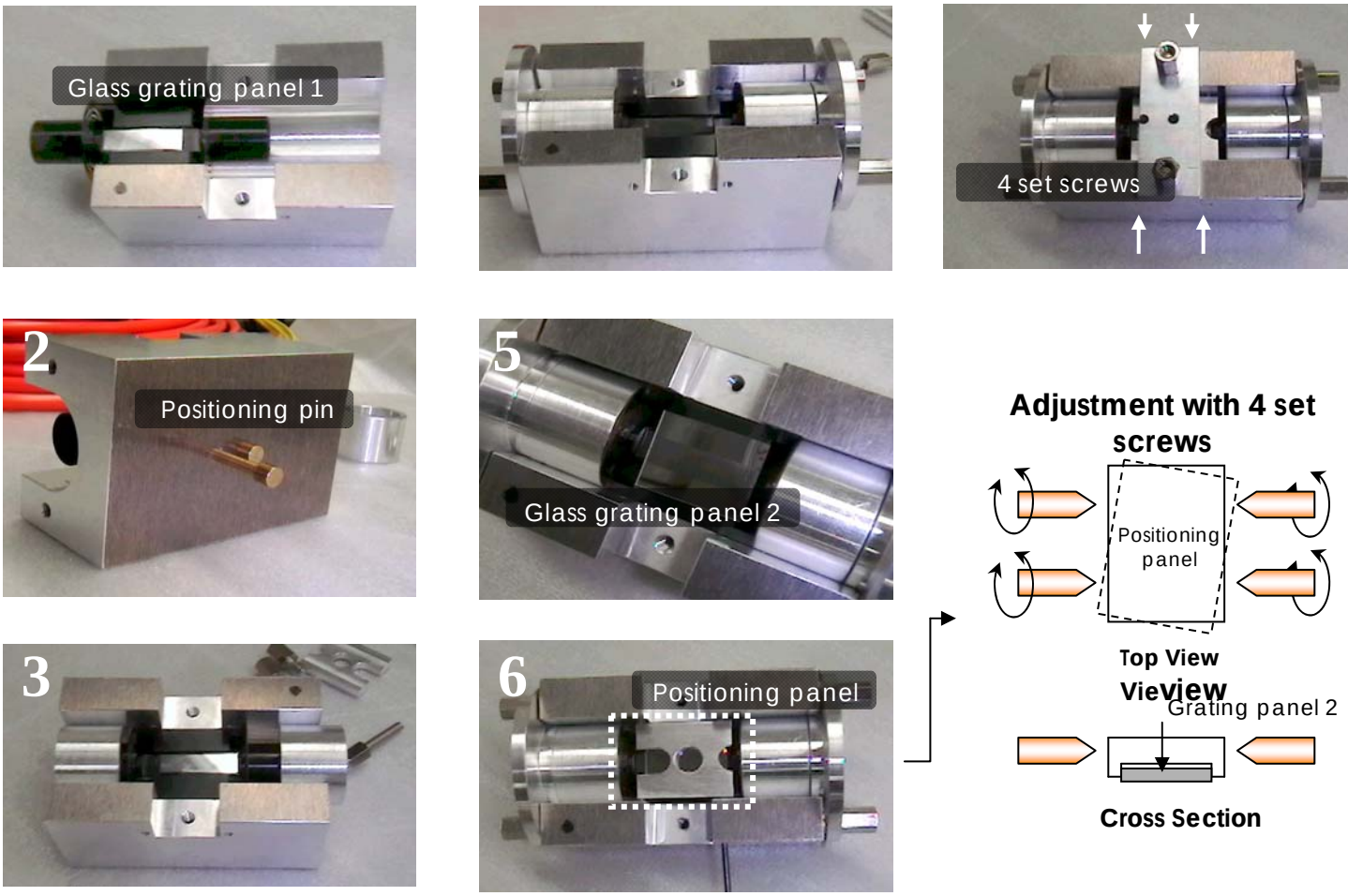

Figure 3. Jig and Process for High-Precision Fabrication and Packaging

3.2.3 Moiré Fringe Signal Processing

We developed algorithms and software to (1) process the raw Moiré fringe signal to the relative displacement and furthermore to the acceleration through an unwrapping process, and (2) further increase the dynamic bandwidth of the accelerometer by applying a lattice filter. All these algorithms were made highly efficient to ensure real time monitoring.

Real-time signal processing is needed to convert the raw Moiré fringe signals to the final acceleration signals. If the focused light source is used to track moiré fringes passing through one point, the transmitted light intensity along the direction of the optical grating rulings is expressed to be sinusoidal with respect to the displacement, as shown in Figure 2. The direction as well as the magnitude of displacement can be measured by using two detectors spaced apart across the fringe profile by a quarter of the fringe width *D*. The two detected light intensity signals are sinusoidal function of displacement having a phase difference of $\pi/4$ with respect to each other, superposed on a DC component as expressed as follows:

$$s_1(t) = C_1 \sin\left(\frac{2\pi x(t)}{d}\right) + C_2$$

$$s_2(t) = C_3 \sin\left(\frac{2\pi x(t)}{d} + \frac{\pi}{4}\right) + C_4 = C_3 \cos\left(\frac{2\pi x(t)}{d}\right) + C_4$$

where C_1, C_2, C_3 and C_4 are constants. The above expressions can be normalized as follows;

$$\bar{s}_1(t) = \frac{s_1(t) - C_2}{C_1} = \sin\left(\frac{2\pi x(t)}{d}\right)$$

$$\bar{s}_2(t) = \frac{s_2(t) - C_4}{C_3} = \cos\left(\frac{2\pi x(t)}{d}\right)$$

The relative displacement $x(t)$ can be obtained by unwrapping the two signals as follows;

$$x(t) = \frac{d}{2\pi} unwrap\left(\arctan\left(\frac{\bar{s}_1(t)}{\bar{s}_2(t)} \right) \right) \qquad (6)$$

Finally, relationship in Eq. 4 is used to convert the displacement into the acceleration.

3.2.4 Dynamic Compensatory Filter

A compensatory filter was developed in this project to further broaden the dynamic measurement range of the sensor. For the single-degree-of-freedom pendulum inside the sensor head, the relative displacement between the mass and the sensor casing (or between the pair of gratings) is measured with a sampling period of ΔT:

$$U_1, U_2, \ldots, U_{n-1}, U_n, U_{n+1}, \ldots$$

This displacement time history can be transformed in an acceleration time history (X) by using the simple relation $X = U \cdot \omega_0^2$:

$$X_1, X_2, \ldots, X_{n-1}, X_n, X_{n+1}, \ldots$$

Assume that a compensated acceleration time history (Y) is as follows;

$$Y_1, Y_2, \ldots, Y_{n-1}, Y_n, Y_{n+1}, \ldots$$

In this case, if V is a hypothetical displacement time history for the compensated system, there is the relation $Y = V \cdot \omega_1^2$ where ω1 is a hypothetical natural frequency. The external acceleration can then be expressed in two ways, by using the recorded displacement and the compensated displacement:

$$\begin{aligned} \ddot{U} + 2\omega_0\zeta_0\dot{U} + \omega_0^2 U &= -\ddot{U}_o \\ \ddot{V} + 2\omega_1\zeta_1\dot{V} + \omega_1^2 V &= -\ddot{U}_o \end{aligned} \tag{7}$$

where ζ_1 is a hypothetical damping ratio.

In Eq.7, $\ddot{U}$, $\dot{U}$, $\ddot{V}$ and $\dot{V}$ can be obtained by numerical methods. A forward difference, a backward difference and a central difference can be applied to Eq.5. The final equation is expressed as follows;

$$\begin{aligned} &\frac{U_n - 2U_{n-1} + U_{n-2}}{\Delta T^2} + 2\omega_0\zeta_0 \frac{U_n - U_{n-2}}{2\Delta T} + \omega_0^2 U_n \\ &\qquad = \frac{V_n - 2V_{n-1} + V_{n-2}}{\Delta T^2} + 2\omega_0\zeta_0 \frac{V_n - V_{n-2}}{2\Delta T} + \omega_0^2 V_n \end{aligned} \tag{8}$$

If parameters determined in the following Eq. 9 are applied to Eq. 8,

$$\begin{aligned} &\lambda_0 = \omega_0 \cdot \Delta T, \quad \lambda_1 = \omega_1 \cdot \Delta T \\ &K_0 = \frac{\zeta_0}{\lambda_0}, \quad L_1 = \frac{\zeta_1}{\lambda_1} \\ &K_0 = \frac{1}{\lambda_0^2}, \quad K_1 = \frac{1}{\lambda_1^2} \end{aligned} \tag{9}$$

Then the following equation can be obtained;

$$\frac{\lambda_o^2}{\Delta T^2}\left[(1+K_0+K_1)U_n - 2k_1U_{n-1} + (K_1-K_0)U_{n-2}\right] = \frac{\lambda_1^2}{\Delta T^2}\left[(1+L_0+L_1)V_n - 2L_1V_{n-1} + (L_1-L_0)V_{n-2}\right] \quad (10)$$

Based on the relations of $X = U \cdot \omega_0^2$ and $Y = V \cdot \omega_1^2$, the following equation can be derived;

$$(1+K_0+K_1)\cdot\left[X_n - \frac{2k_1}{1+K_0+K_1}X_{n-1} + \frac{K_1-K_0}{1+K_0+K}X_{n-2}\right] = (1+L_0+L_1)\cdot\left[Y_n - \frac{2L_1}{1+L_0+L_1}Y_{n-1} + \frac{L_1-L_0}{1+L_0+L_1}Y_{n-2}\right] \quad (11)$$

Finally, the compensated acceleration (Y) can be expressed as follows;

$$Y_n = -a_1 \cdot Y_{n-1} - a_2 \cdot Y_{n-2} + \varphi \cdot \left[X_n + b_1 \cdot X_{n-1} + b_2 \cdot X_{n-2}\right] \quad (12)$$

where a_1, a_2, b_1 and b_2 are determined as follows;

$$a_1 = \frac{-2L_1}{1+L_0+L_1}, \quad a_2 = \frac{L_1-L_0}{1+L_0+L_1}$$
$$b1 = \frac{-2K_1}{1+K_0+K_1}, \quad b_2 = \frac{K_1-K_0}{1+K_0+K_1}$$
$$\varphi = \frac{1+K_0+K_1}{1+L_0+L_1}$$

By using the actual acceleration time history and Eq.12, the compensated acceleration can be easily obtained. As a result, we can shift the natural frequency and the damping ratio of the fiber optic accelerometer sensor to expand the dynamic bandwidth of the acceleration. In this study, we designed the hypothetical natural frequency to be 50 Hz and the hypothetical damping ratio 0.707. Figure 4 compares the dynamic deformation

factors (defined in Eq. 4) with and without the compensatory filter applied. By using the compensatory filter, the measured acceleration is successfully converted into the hypothetical acceleration that can be measured by the hypothetical accelerometer with the designed hypothetical natural frequency and damping ratio. As a result, the actual fiber optic accelerometer can measure accelerations up to 30 Hz with a maximum error less than 5% by using the compensatory filter. As an example, Figure 5 shows 23 Hz sinusoidal acceleration measured by the prototype fiber optic accelerometer with and without the compensatory filter, in comparison with that measured by the reference sensor. The compensated acceleration agrees much better with the reference signal than the uncompensated one.

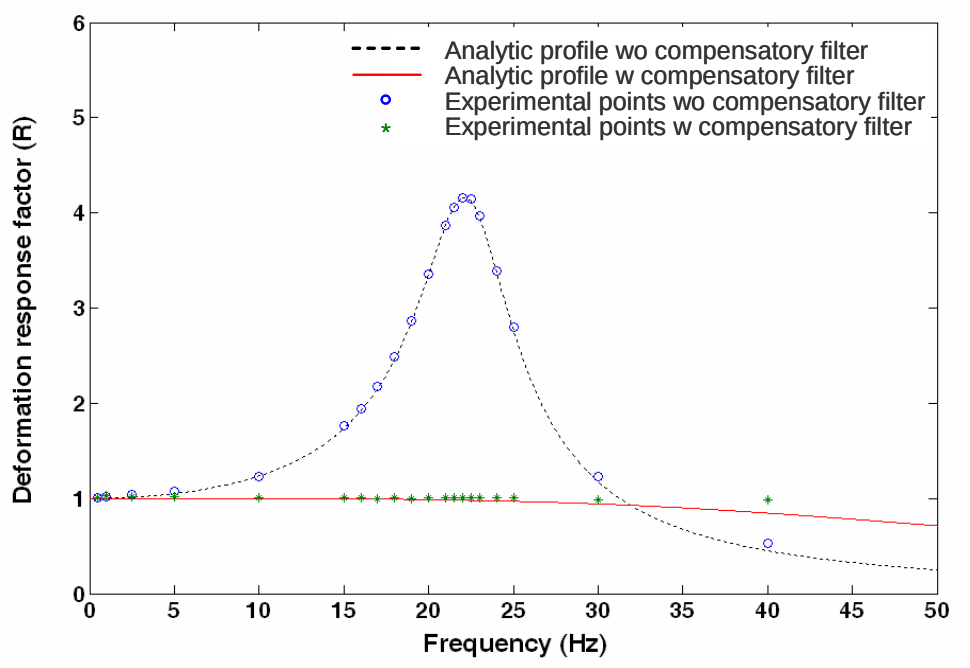

Figure 4. Deformation Response Factors with and without Compensatory Filter

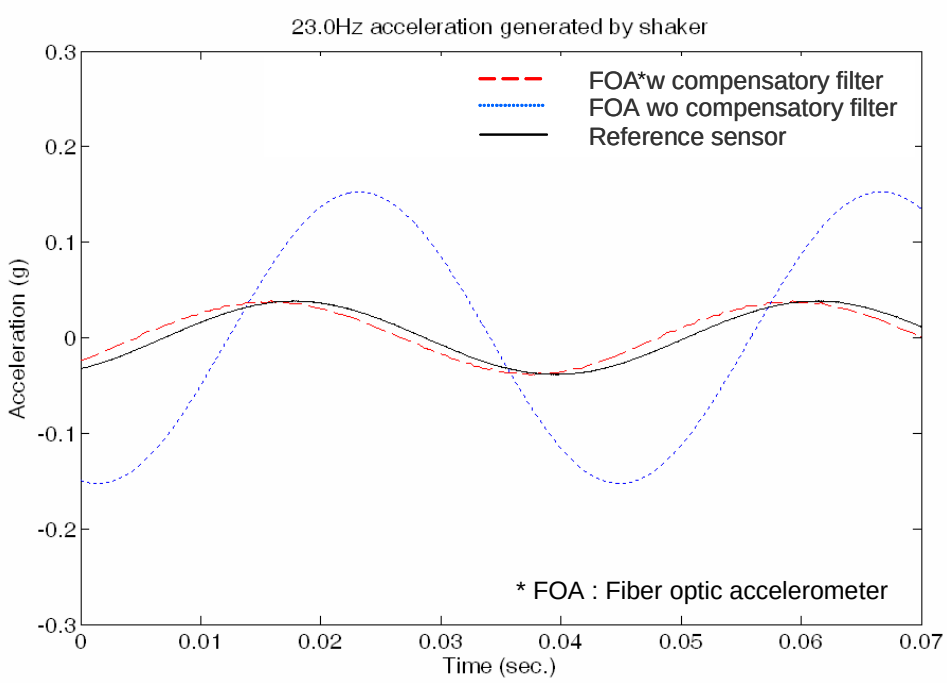

Figure 5. Accelerations with and without Compensatory Filter

With the same algorithm used for the acceleration compensatory filter as described above, the phase lag ϕ between the actual acceleration and the measured acceleration is plotted in Figure 6, which is approximately the same phase lag when the damping ratio is 0.7. As shown in Fig. 6, the phase lag is proportional to the excitation frequency, and thus φ / ω is essentially constant. Recall Eq. (5) in Section 2, the time delay between the actual acceleration and the measured acceleration is constant, independent of the frequency contents of the actual acceleration.

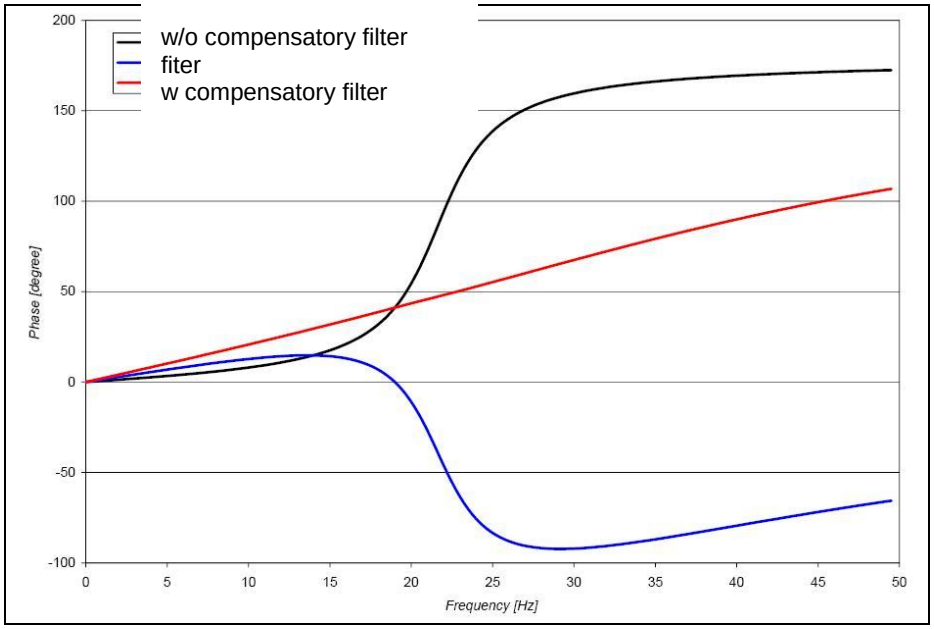

Figure 6. Phase Lag with and without Compensatory Filter

3.2.5 Prototype Accelerometer System

In order to investigate the technical feasibility of the proposed optical fiber accelerometer, a proof-of-concept prototype sensor system was first fabricated based on the conceptual design and key parameter values determined in Section 3.2.1 and using the manufacturing process and techniques developed in Section 3.2.2. For the sensor head, we fabricated a pair of glass panels with glass in which fine gratings with a 50 lines/mm pitch was applied and two pairs of optical collimators. The specifications of the grating panels and the lenses are shown in Table 3.

Table 3. Specifications of the Key Optical Components

Optical Fiber	Graded index multimode fiber (62.5/125 μm)
Lens	F=1.81 mm GRIN
Grating Pitch	d (period) = 200 μm

Meanwhile, we designed and fabricated key mechanical parts for the sensor head including a pair of springs, dampers, a mass, and a case, as shown in Figure 7.

Figure 7. Fabricated Mechanical Parts for Prototype Accelerometer

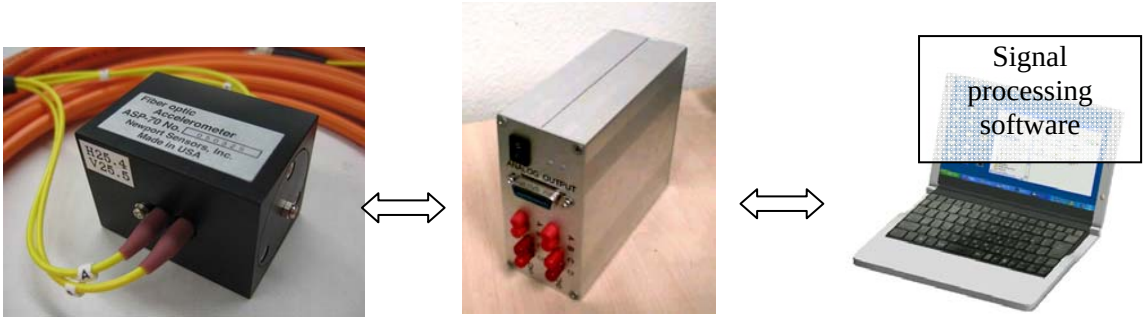

Figure 8. Prototype Accelerometer System

Finally, a multi-channel accelerometer system was prototyped. This system includes multiple sensor heads, one multi-channel control unit, and a PC, as shown in Figure 8. The prototype sensor head has a dimension of 33*33*48 mm and a weight of 150g. The sensor head consists of a pendulum with a mass, a spring, and a damper, together with two glass gratings and two pairs of optical fibers. The sensor head is linked to the control unit by the two optical fibers. The control unit provides the light source to each sensor head through two optical fibers and detects the intensity variation of the light transmitted through the two optical gratings. Totally sixteen LEDs and sixteen photo diodes are used in this unit. A rechargeable battery is included in the unit for portability. The control unit has a simple structure and the cost is much lower than many of the existing fiber optic sensor systems.

On the other hand, a computer software for controlling the sensor interrogation and signal acquisition and processing was developed using visual C++. The software incorporates the raw Moiré fringe signal processing and the dynamic compensatory filtering algorithms described earlier. Figure 9 shows the frame of the developed software. We can control the parameters of the compensatory filter for each sensor as well as those of the data acquisition system up to eight sensors simultaneously.

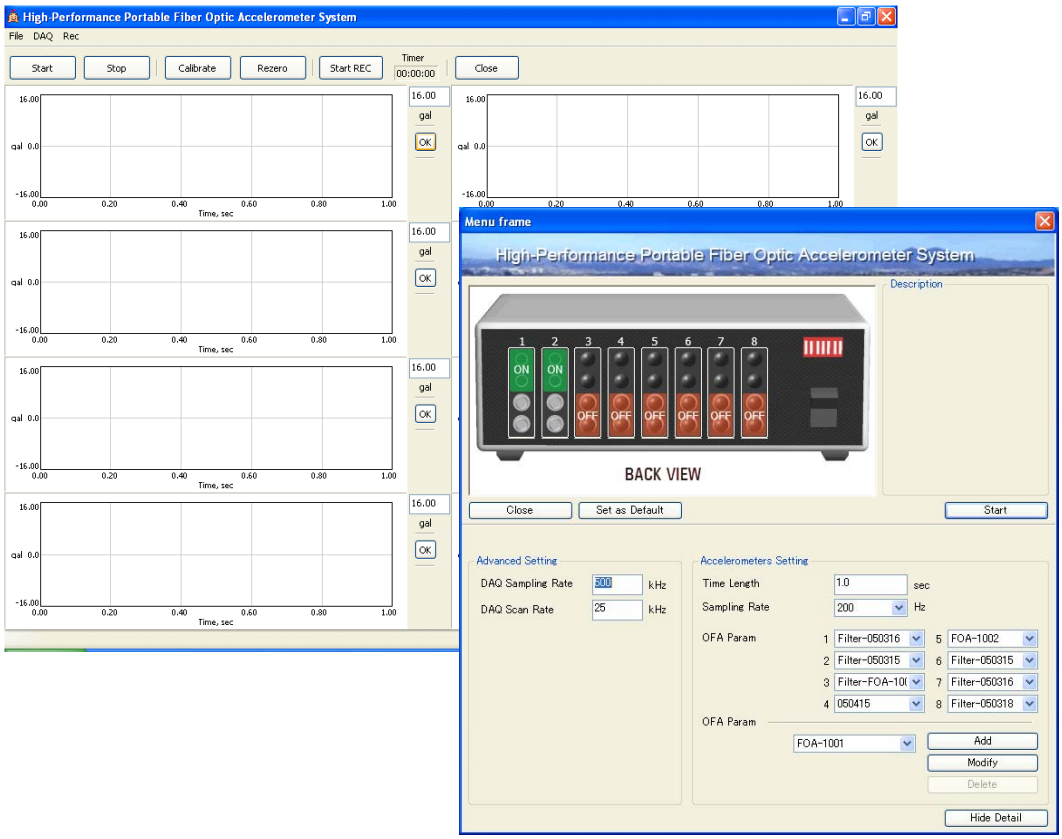

Figure 9. Control Software for Signal Processing in Real Time

3.2.6 Sensor Characterization Tests

The natural frequency and the damping ratio of the fiber optic accelerometer should be identified in order to convert the raw optic signals to the acceleration, as shown in Eq. 4. The frequency-response curve of the prototype accelerometer was experimentally obtained, by mounting the accelerometer, together with a high-performance reference sensor on a shaking table. The shaking table was excited by sinusoidal signals at selected frequencies covering a large range and the amplitude of the steady-state acceleration was measured. A frequency-response curve in the form of deformation response factor (ratio

between the relative displacement of the prototype accelerometer $D_{response}$ and the acceleration of the reference sensor A_{excite}) was then plotted as a function of the excitation frequency ω, from which the natural frequency and the damping ratio of the pendulum system inside the sensor head was determined.

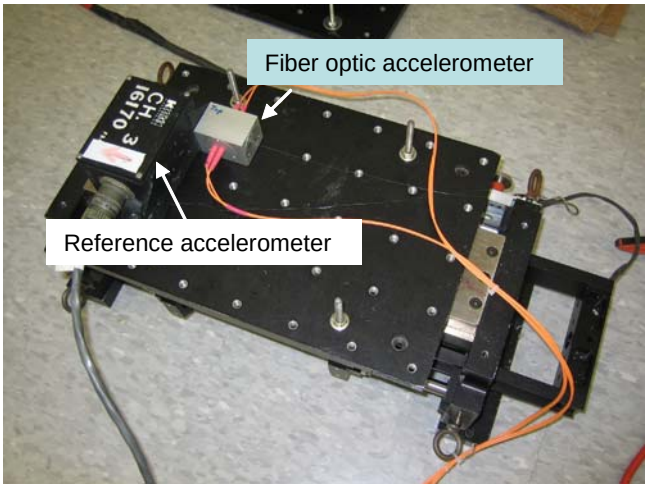

Figure 10. Experimental setup for characterization test

The prototype fiber optic accelerometer and a reference sensor (Kinemetrics, FBA-11) were fixed to the shaking table (APS-Dynamics, model 113) as shown in Figure 10. The reference sensor is an electric sensor equipped with a pendulum and a servo control circuit to achieve a large bandwidth (DC to 200Hz). A fixed-sine function generator was used to control the shaking table. The frequencies of the excitation signals were selected as 0.5Hz, 1.0Hz, 2.5Hz, 5.0Hz, 10.0Hz, 15.0Hz, 16.0Hz, 17.0Hz, 18.0Hz, 19.0Hz, 20.0Hz, 21.0Hz, 21.5Hz, 22.0Hz, 23.0Hz, 24.0Hz, 25.0Hz, 30.0Hz and 40.0Hz. Each test was performed five times in order to average out the errors in data acquisition and to check the standard deviation in the data.

Figure 4 in Section 3.2.4 plots the deformation response curve *R* defined as ($\left|D_{response} / A_{excited}\right| \cdot \omega_0^2$) based on the testing results, in comparison with the theoretical curve discussed in Section 2. By fitting the experimental data to the theoretical curve, the natural frequency of the prototype is 22.45 Hz and the damping ratio is 0.12.

Again, by using the compensatory filter as described in Section 3.2.4, the natural frequency of the sensor can be hypothetically extended to 50 Hz and the damping increased on 70%. As a result, this fiber optic accelerometer can measure accelerations up to 30 Hz by using the compensatory filter as demonstrated in Figure 4 of Section 3.2.4, in which both experimental and theoretical curves are presented.

As shown in the figure, the experimental results fit very well with the theoretical ones with or without the compensatory filter, indicating that the high-accuracy of the fiber optic sensor system developed in this study. Also, a high repeatability of the sensor data was observed during the shaking table tests, indicating the high reliability of the sensor.

3.2.7 Vibration and Seismic Shaking Table Tests

The performance of the fiber optic accelerometer system developed in this study was extensively evaluated in (1) a vibration test of a concrete bridge slab model in the Structural Engineering Laboratory. University of California, San Diego (UCSD), and (2) a seismic shaking table test of concrete bridge models at University of Nevada, Reno (UNR).

In the UCSD tests, the concrete slab structure was laid down on a stage as shown in Figure 11. Two loading poles were installed to apply vertical static loads at two different locations on the slab, simulating vehicle loading. The static loading was

gradually increased to damage the slab to different levels. At different damage level, a shaker installed at the top of the slab excited the slab with low-amplitude white noise. The response acceleration was measured to demonstrate the change in dynamic characteristics caused by the damage. Four fiber optic accelerometers were installed on the top surface of the slab, together with 28 piezo-ceramic accelerometers (PZT, PCB co., Model-3701D2FA20G)), Figure 12 shows the locations of these sensors as well as the static loading and dynamic shaking. All of sensors measured the accelerations in vertical direction. The fiber optic accelerometers were connected to the electric control unit and furthermore to the laptop computer for data acquisition and converting the raw data to accelerations through the real-time processing software.

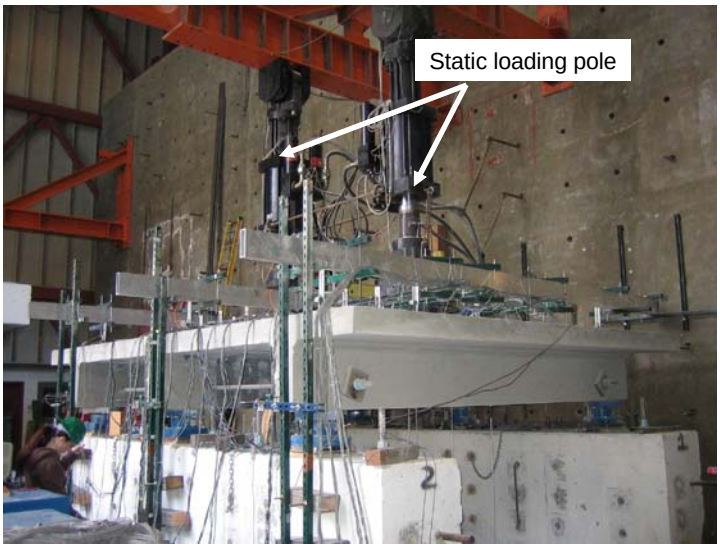

Figure 11. Concrete Bridge Slab Structure

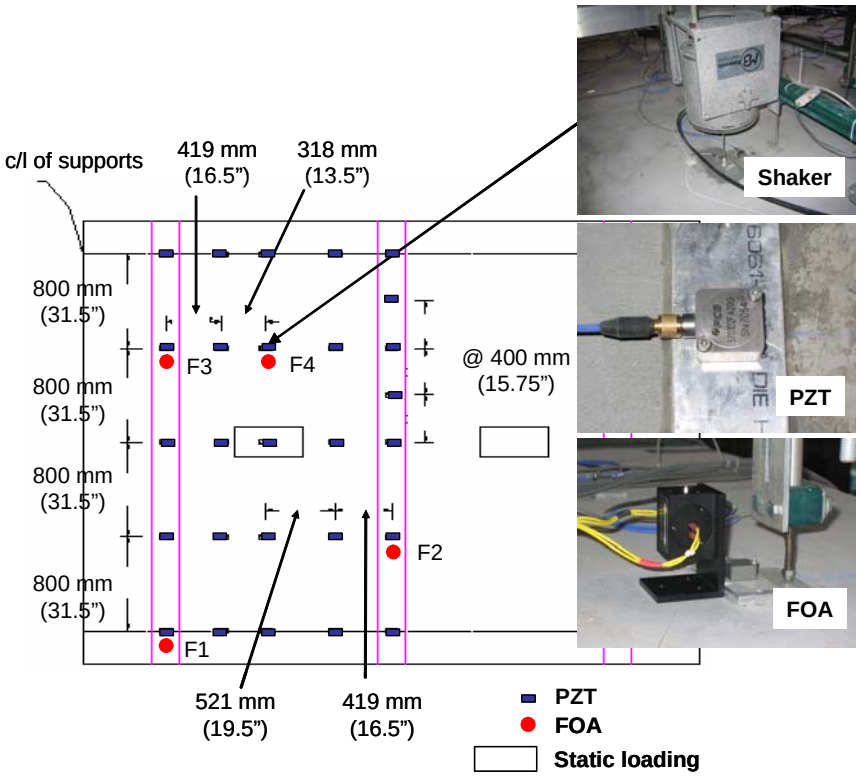

Figure 12. Locations of Fiber Optic Accelerometers (FOA) and Piezo Transducers (PZT)

Table 4 shows the static loading steps. At each loading step, a static load was gradually applied to the slab up to a certain level and then gradually removed. The loading level was increased to cause the slab to damage to different levels. The slab failed at the step 6-2 where the loading level reached 210 kips. After each static loading step, the slab was excited with white noise generated by the shaker for 250 seconds. The PZT and the fiber optic accelerometers measured the accelerations during the slab's excitation.

Table 4. Static loading condition

Tasks	Step name	Loading Steps [kips] (per each loading pole)
Baseline	Step0-2	0->**24**->0
3	Step3-2	0->**120**->0
6	Step6-2	0->**210**->0

The concrete slab structure has several vibration modes. We measured the vibration up to the 4th mode, which is approximately 100Hz. In order to measure vibration up to 100Hz, we increased the dynamic bandwidth of he fiber optic accelerometers by using the compensatory filter described in Task 3. In this experiment, 200Hz and 0.707 were chosen as the hypothetical natural frequency and the damping ratio respectively for the expanding the dynamic bandwidth up to 120Hz. Figure 13 shows the comparison of the frequency responses measured by the fiber optic accelerometer and the PZT transducer. Excellent agreement is demonstrated.

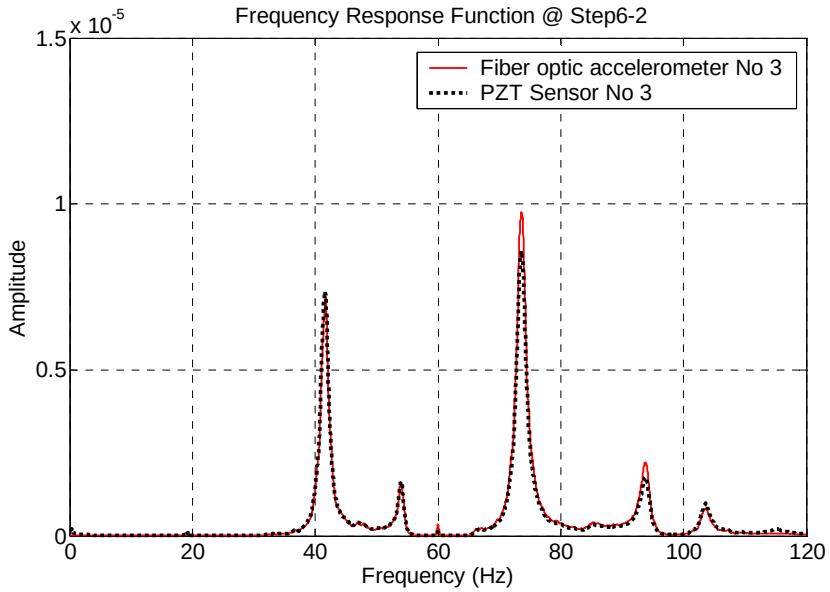

Figure 13. Comparison of Frequency Responses Measured by the Fiber Optic and PZT Accelerometers

Figure 14 shows a portion of the acceleration time histories measured by the fiber optic accelerometer (# F3 in Figure 11) after three different loading steps. The first acceleration was measured after the loading step 0-2 and the second and the third one were after the loading step 3-2 and 6-2.

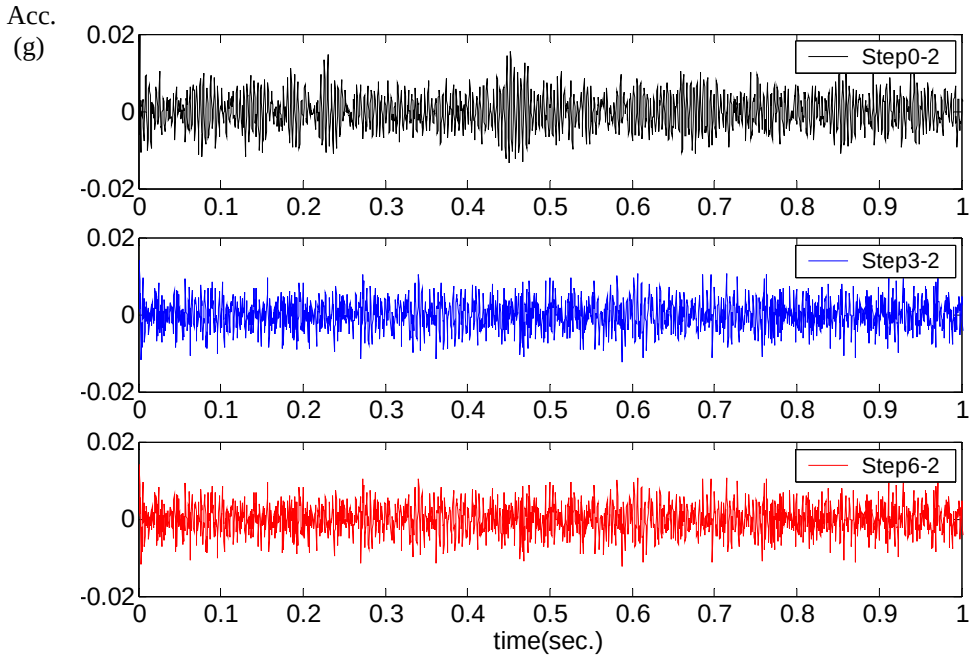

Figure 14. Accelerations Measured by Fiber Optic Accelerometer

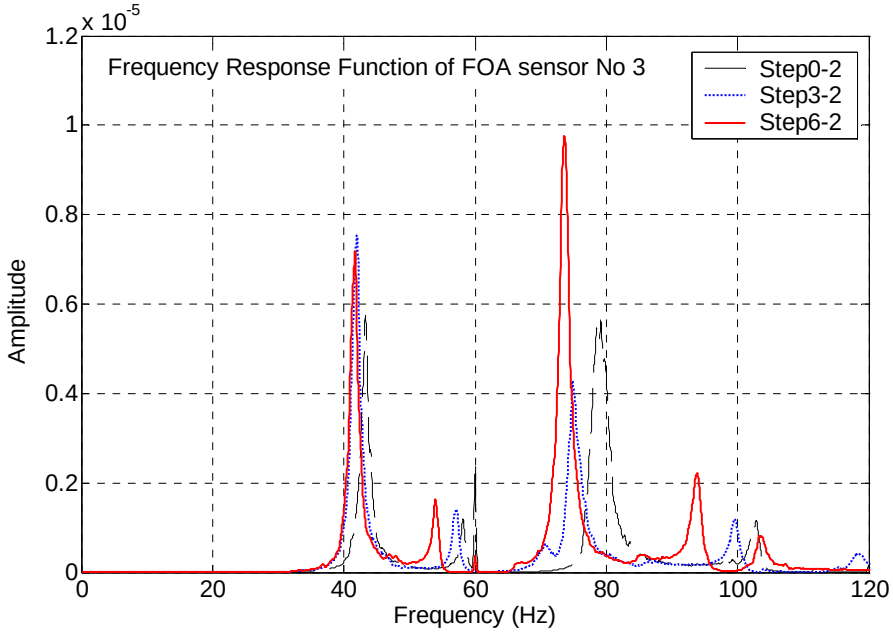

Figure 15. Changing of Dynamic Characteristics Depending on Loading Steps

The frequency responses of these three accelerations are indicated in Figure 15. As shown in the figure, the peak values showing natural frequencies at four modes all shifted toward left (decreased) as the loading level increased. This implies that the stiffness of the slab decreased as the static loading caused damage to the slab structure.

Table 4 summaries the change in natural frequencies of the first four modes caused by the structural damage. The first natural frequency was reduced by 2.96% after the loading step 3-2, and then further reduced by 3.58% after the loading step 6-2. The higher modes exhibited more frequency reduction than the first mode after the loading step 6-2. The fiber optic accelerometer system successfully measured the vibration responses in real time and identified the change in natural frequencies caused by the structural damage at different levels.

Table 4. Change in Natural Frequencies Caused by the Structural Damage

Vibration Mode	Baseline Step0-2 @ 24 kips (Hz)	Step3-2 @ 120 kips (Hz)	Step6-2 @ 210 kips (Hz)	Shift at Step3-2 (%)	Shift at Step6-2 (%)
1	43.27	41.99	41.72	-2.96	-3.58
2	58.14	57.13	53.96	-1.74	-7.19
3	79.19	74.86	73.61	-5.47	-7.05
4	102.84	99.55	93.81	-3.20	-8.78

In the shaking table tests at UNR, the fiber optic accelerometers were compared with high-performance force-balance seismic accelerometers (I6083) made by Kinemetrics as reference sensors. Figure 16 is a photo of the bridge bent model and the fiber optic sensor, together with the reference sensor. Figure 17 shows the sensor

locations. Figure 18 compares the seismic response accelerations measured at the base of the bent respectively by the fiber optic accelerometer and the reference sensor. Excellent agreement is observed in both the time domain and the frequency domain, demonstrating the high performance of the fiber optic accelerometer developed in this project.

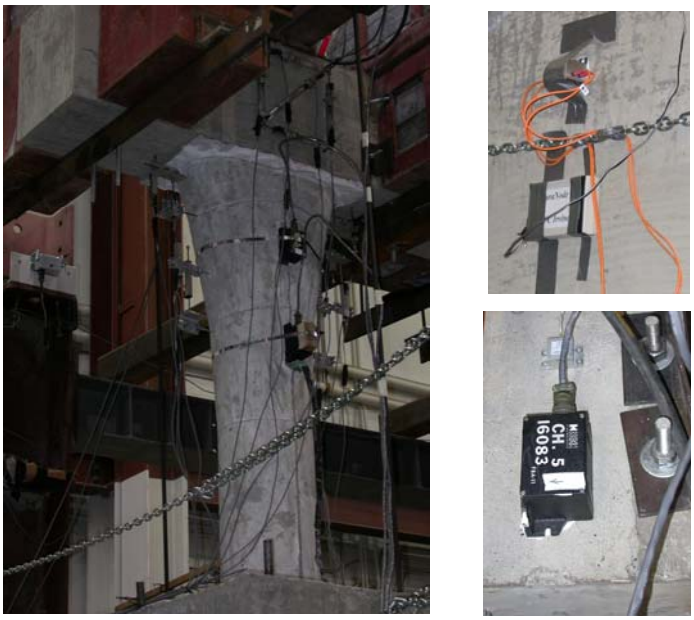

Figure 16 Performance Evaluation Through Seismic Shaking Table Tests

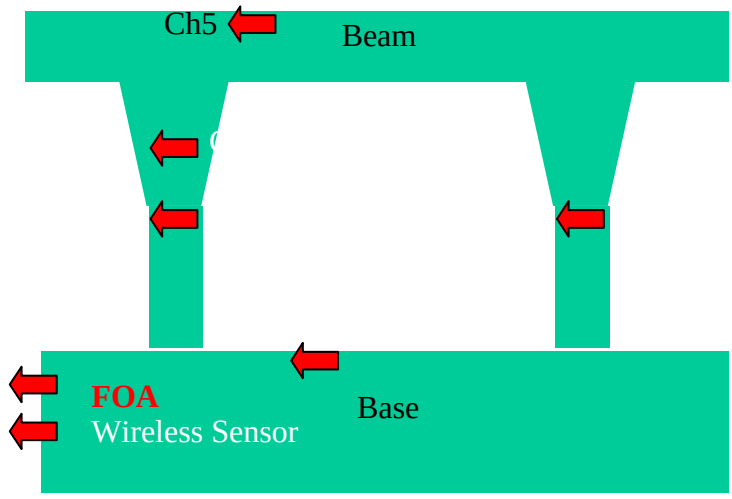

Figure 17 Sensor Locations in Seismic Shaking Table Tests

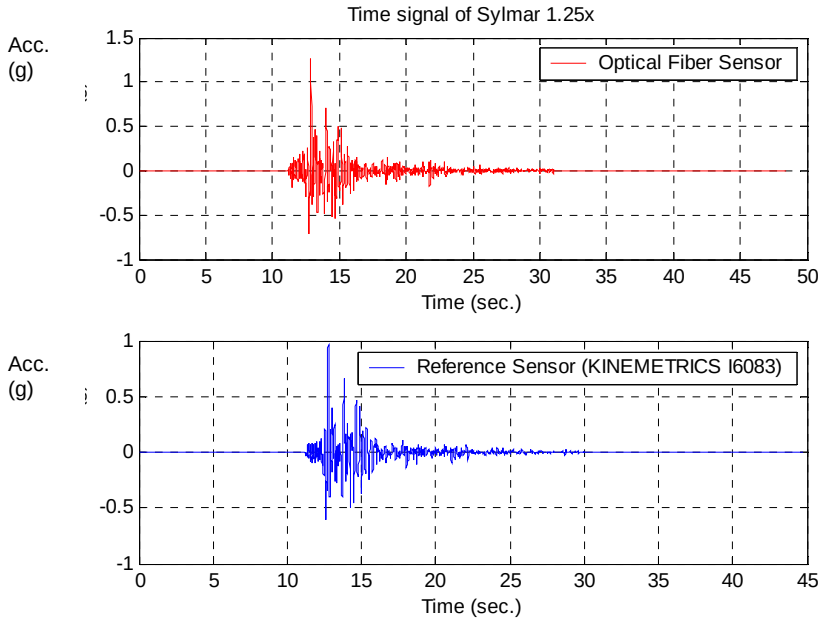

(a) Time Domain

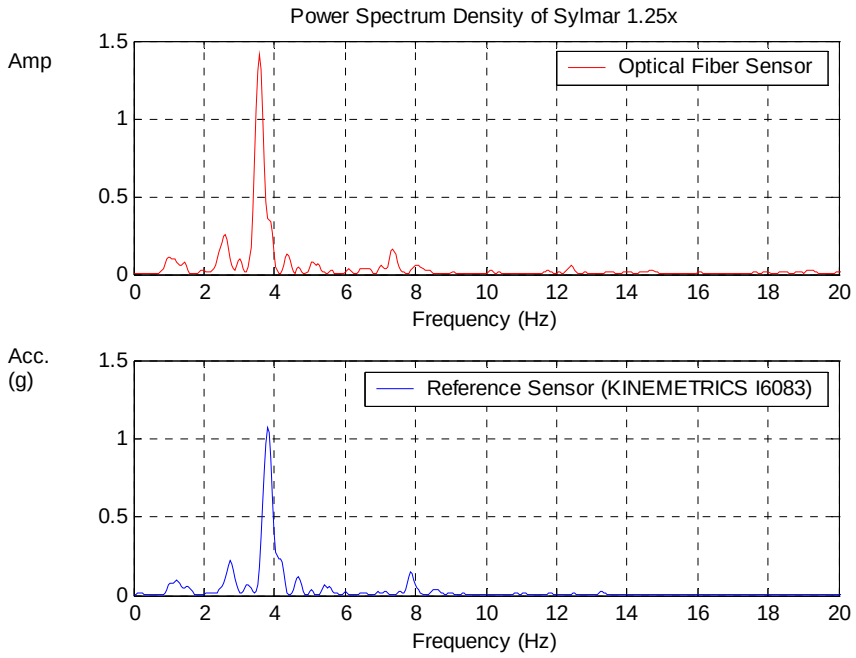

(b) Frequency Domain

Figure 18 Comparison of Seismic Responses Measured by the Fiber Optic and Conventional Accelerometers

3.2.8 Field Tests on Two Bridges and One Building

The performance of the fiber optic accelerometer system developed in this study was further evaluated in the field to measure traffic induced vibration at (1) the Painter Street bridge in Eureka, CA, and the (2) West St. On-Ramp in Anaheim, CA. Figure 19 shows the tests at the Painter St. Overcrossing and Fig. 20 at the West St. On-Ramp.

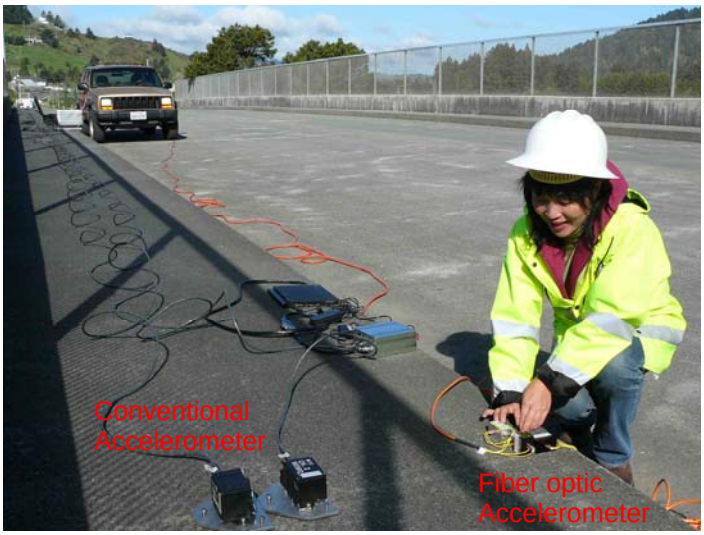

Figure 19 Test at Painter St. Overcrossing

Figure 20 Test at West St. On-Ramp

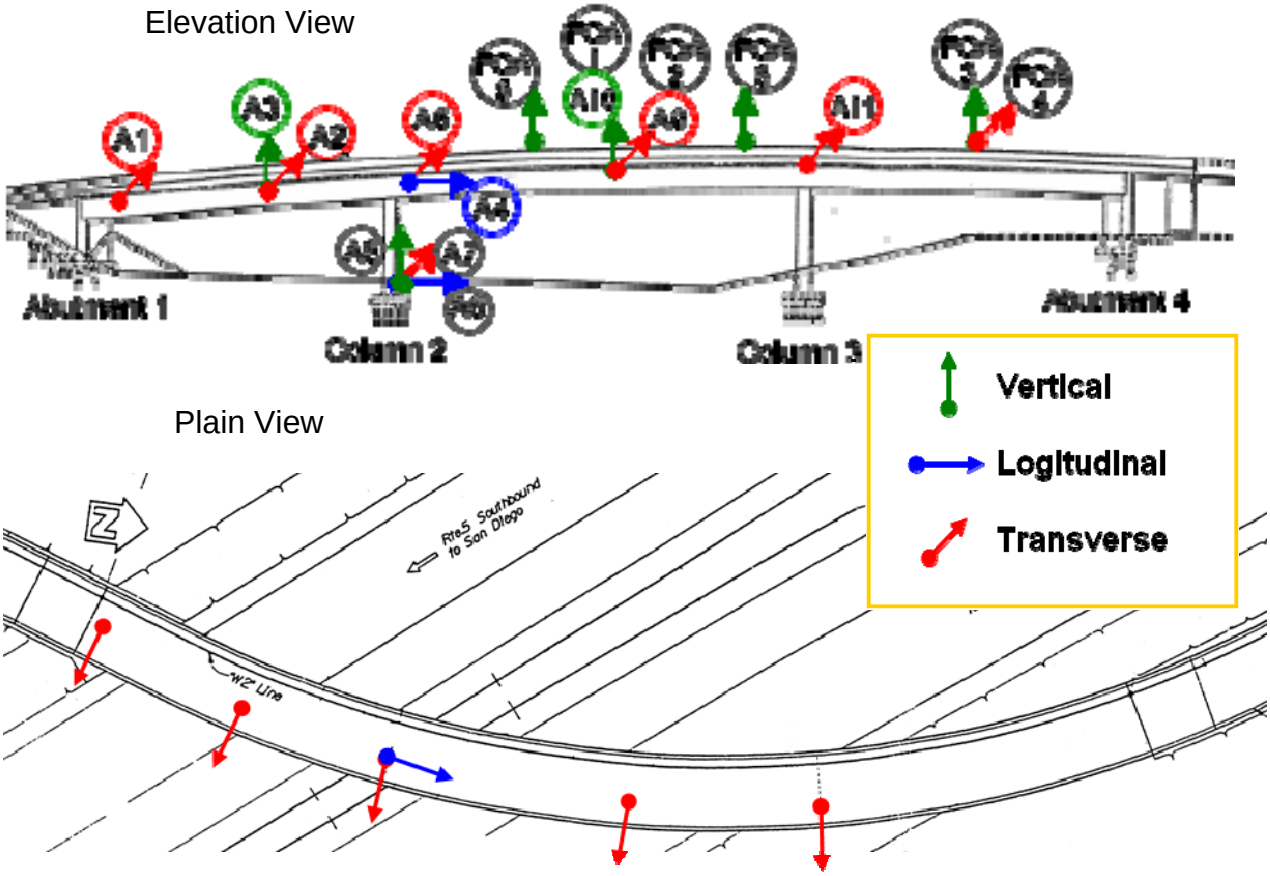

Figure 21 Sensor Layouts at West St. On-Ramp

Under the in-kind support of Caltrans, the test of the West St. On-Ramp was conducted with traffic control using a fully loaded water truck. The three-span curved concrete box-girder bridge has a total length of 497 feet. Eleven conventional force-balance high-performance accelerometers (made by Tokyo Sokushin, Inc.) are permanently installed on the bridge. Four fiber optic accelerometers developed in this project were installed at the same locations of some of the conventional accelerometers for the comparison purposes. The sensor layouts are shown in Fig. 21, in which A denotes conventional accelerometers while FOA the fiber optic accelerometers.

The water truck applied a sudden breaking force when traveling at the middle of the mid-span. Figure 22 compares the accelerometers measured by the conventional (permanently installed) accelerometer A 9 and the fiber optic accelerometer (FOA 2). Excellent agreement is observed.

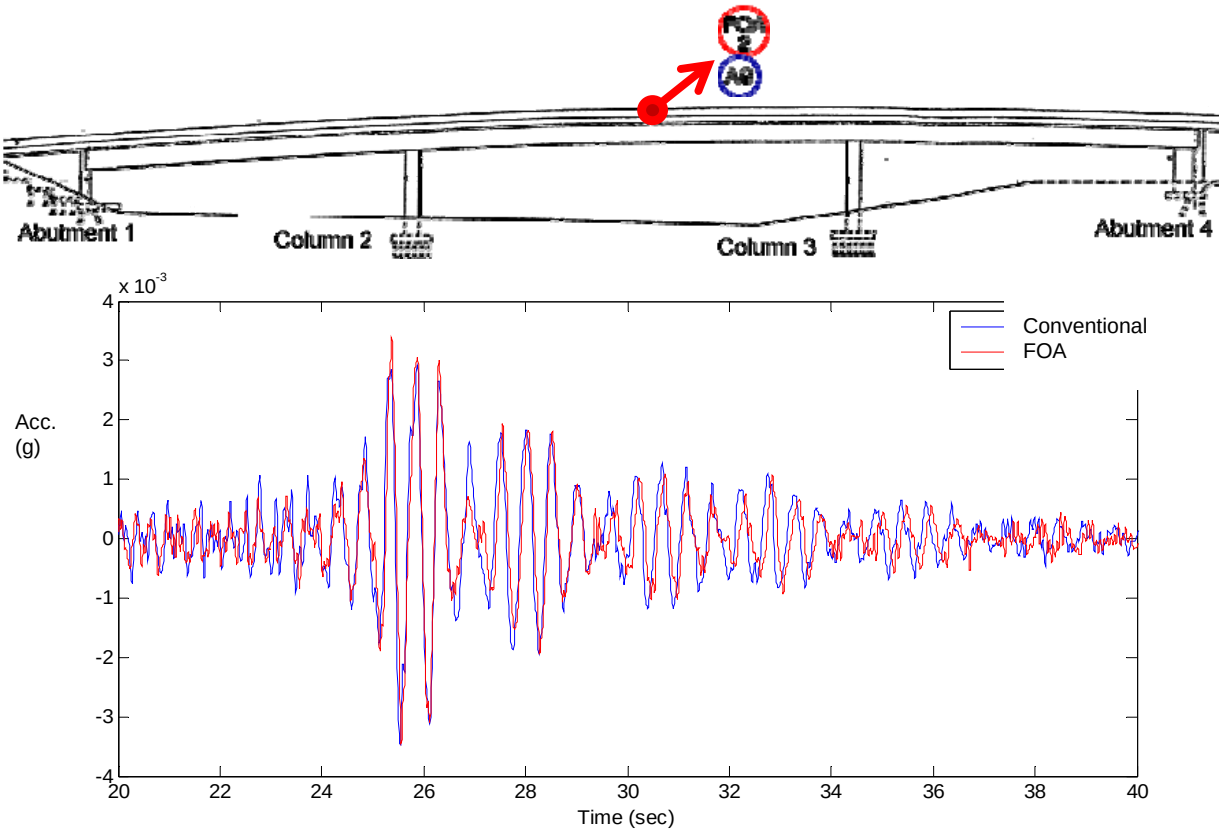

Figure 22 Accelerations Measured by Conventional and Fiber Optic Accelerometers (FOA) under Breaking Test

Table 5 compares the natural frequencies of the West St. On-Ramp identified by all of the conventional and all of the fiber optic accelerometers under the breaking test. They agree with each other well, demonstrating the high performance of the fiber optic accelerometers comparable with the force-balance seismic accelerometers.

Table 5. Identified Natural Frequencies of West St. On-Ramp (Hz)

Accelerometer	Mode 1	Mode 2	Mode 3	Mode 4
Conventional	1.86	2.25	2.64	3.41
Fiber Optic	1.89	2.26	2.70	3.36

The field tests at the two bridge sites also demonstrated another two advantages of the fiber optic sensor over the conventional force-balance accelerometers. One is the ease of installation and cabling due to the small size and lightweight of the sensor heads and fiber optic cables, and the other is the immunity of the fiber optic sensors to the electromagnetic noise. Due to the lightweight of the sensor head, the fiber optic accelerometers can be easily glued to the surface of a structure, as shown in Fig. 23.

It is noted that field test of the fiber optic accelerometers at the West St. On-Ramp was reported by the National Public Radio (NPR). Figure 24 is a photo of the PI with the NPR reporter, Ms. Susan Valot, at the bridge.

Figure 23 Installation of Fiber Optic Accelerometer

Figure 24 Interview by the National Public Radio at the Bridge Testing Site

In addition to the field tests at the two bridge sites, the fiber optic accelerometer system was also tested on a four-story office reinforced concrete building (shown in Fig. 25) in Orange County, CA, to measure its ambient vibration. High-performance force-balance accelerometers were used as reference sensors. The figure also compares the ambient vibrations measured on the second floor of the building by the fiber optic accelerometer and the reference sensor in both time and frequency domains. They show excellent agreement. This field test demonstrates the capability of the fiber optic accelerometers in measuring low-amplitude acceleration (in the order of 10^{-4}g) with a sufficient resolution.

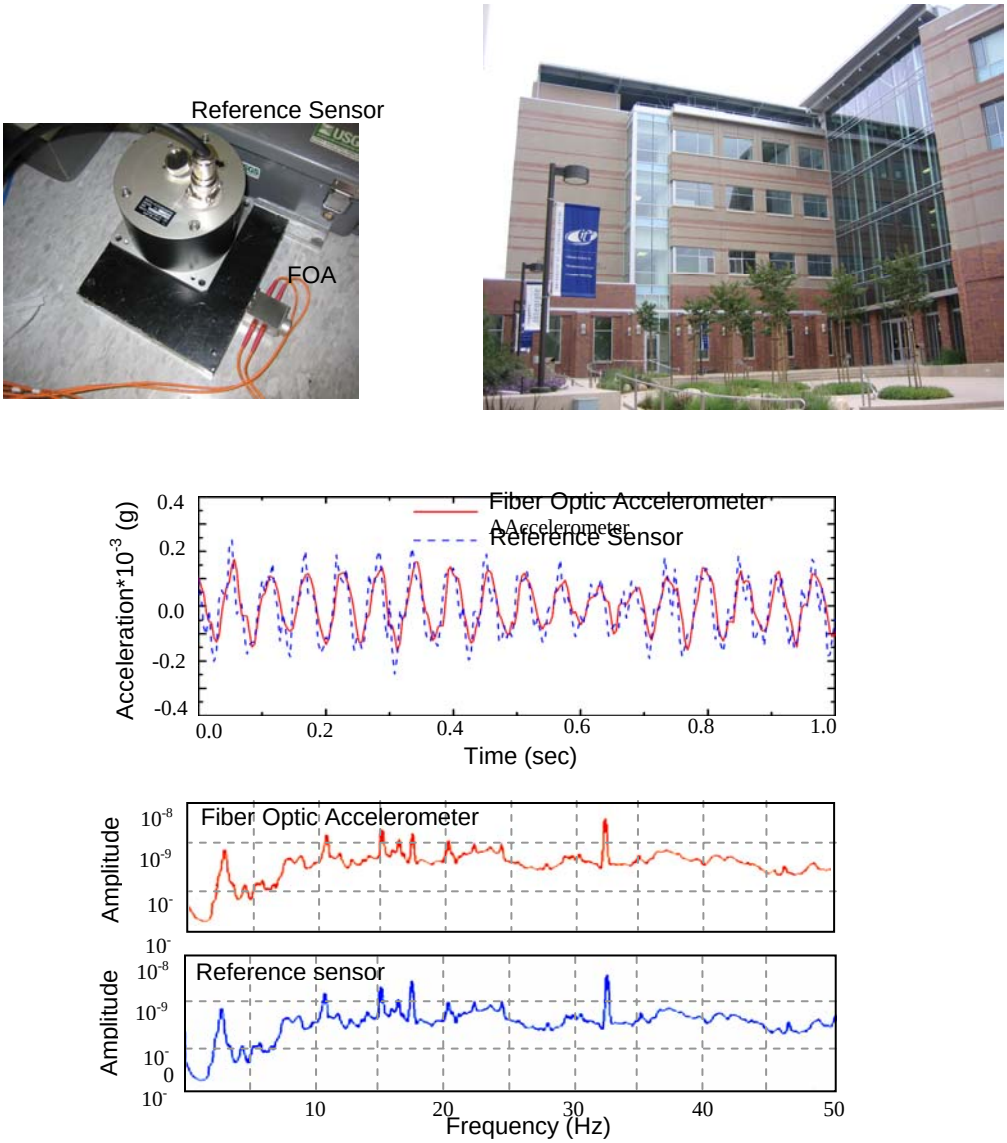

Figure 25 Field Test To Measure Ambient Vibration of a Building

3.2.9 Evaluation of Cost and Commercial Feasibility

The cost and commercial feasibility was evaluated in order to facilitate a quick transfer of the IDEA research results to commercial products upon the completion of the IDEA project. In the sensor and monitoring market, NSI's fiber optic accelerometer products, while priced comparably to the two conventional electrically wired sensor products, possesses clear advantages deriving from reliance on its optical signal and dielectric materials. As a result, it is safer, cleaner and far less expensive to install. These attributes make the fiber optic accelerometer system an ideal product to monitor high-risk sites such as bridges with oil and gas pipelines, where the risk of electrical spark and high electromagnetic interference (EMI) has prevented the application of electrically wired sensors.

The following is the information of the two competitors:

Kinemetrics, Inc.

Kinemetrics was established in 1969 and is based in Pasadena, California and produces products for monitoring bridges, dams, structures, seismic arrays and networks, as well as systems for the nuclear power industry. Their instruments are used to monitor the seismic safety of many of the world's most famous structures, including New York's Statue of Liberty, San Francisco's Golden Gate Bridge, Egypt's Sphinx, Athen's Parthenon and the Taj Mahal. In 1991 Kinemetrics was acquired by OYO Corporation of Japan. Kinemetrics also has an office in Switzerland.

It is difficult to estimate the firm's revenues but the website states the Company has 45 representatives and a service department.

Tokyo Sokushin Co. Ltd.

Tokyo Sokushin was founded in 1970 and currently has 50 employees and annual revenue of about $11 million. Its basic products include seismometers and seismographs, digital recorders for earthquake and wind monitoring and ambient vibration monitoring systems. It is the leading manufacturer and supplier of low-frequency vibration sensors in Japan. Dr. Feng at NSI has a long-term collaboration and affiliation with Mr. Isamu Yokoi, Founder and CEO of Tokyo Sokushin.

In the laboratory and field tests in the IDEA project, the project team compared the prototype fiber optic accelerometers with the conventional electric sensors made by the two competitors. Table 6 shows the comparison of the NSI fiber optic accelerometer with its competitive products. Based on the analysis, NSI is confident that the future fiber optic accelerometer products will have competitive advantages.

Table 6 NSI Competitive Advantage

Manufacturer	Product	Price	Performance
Kinemetrics, Inc.	Electrical sensors	$2,000 per sensor (incl. control unit or data logger)	Matured technology, stable,
Tokyo Sokushin, Inc.	Electrical sensors	Same as above	Same as above
NSI	Fiber optic sensors	$1,500 - $2,000 per sensor (incl. control unit)	Safe (no electric spark) Clean signal (no EMI) High accuracy & resolution Little signal attenuation Less installation cost Low cost

Note: The cost of electrical cables is much higher than that of optical fiber cables.

4. PLAN FOR IMPLEMENTATION

This IDEA project has successfully developed the novel fiber optic dynamic sensing concept into a high-performance prototype accelerometer system, carried out extensive laboratory and field evaluation tests, and finally investigated its cost and commercial feasibility. The success of the IDEA project has laid a solid foundation for quick technology transfer and commercialization beyond the IDEA project.

The IDEA Advisory Board consisting of potential end users and partners has played an important role in this project, by providing advice on product positioning, partnerships, and market opportunities. In particular, NSI has obtained in-kind support from (1) Caltrans (one of the largest bridge owners in the U.S.) in the field evaluation tests on the two Caltrans highway bridges, and (2) Tokyo Sokushin, Inc. (one of the two major manufacturers of the conventional high-performance force-balance accelerometers) in precision fabrication and packaging of the sensors. These potential early adopters and business partners will be significant recourses for the future manufacturing, marketing and distribution of the sensor products.

NSI plans to commercialize the fiber optic dynamic sensor technology through product development and marketing within one year post IDEA. The company has developed technical specifications and a preliminary design of an 8-channel fiber optic accelerometer system, as shown in Tables 7 and 8.

Table 7. Specifications of Accelerometer

Model	CF-1000
Frequency Range	DC ~ 40Hz
Measurement Range	-3g ~ +3g
Resolution	$1X10^{-5}g$
Cable	Multimode optic fiber cable
Operating Temperature	-30^0C ~ $+40^0C$
Dimension	34X34X48mm
Weight	0.1kg

Table 8. Specifications of Control Unit

Model	CUP-1008
Number of Channels	8
Power Supply	12V rechargeable battery AC-DC selectable
Dimension	280X200X90 mm
Weight	2 kg
Operating Temperature	-30^0C ~ $+40^0C$

The optical fiber accelerometer products will have a broad impact on the safety and security of the nation's highway transportation infrastructure. Due to aging and deterioration, the infrastructure is becoming increasingly vulnerable to natural and man-made disasters including vehicular overloads, accidents, hurricanes, earthquakes, and terrorist attacks. The emerging sensor technology has demonstrated its potential for real-time monitoring of structural integrity of highway bridges. Due to its relative ease of surface mounting on existing structures, vibration sensors such as accelerometers are gaining increasing popularity for structural health monitoring, in comparison with other sensors (such as strain sensors) that require embedment during construction. One of the major obstacles, however, preventing implementation of sensor-based monitoring is the

lack of reliable, easy-to-install, and cost-effective sensors that are suited for and can be densely deployed on highway bridges. Commercially available (mainly electric-type) sensors use electric cables for signal transmission and power supply that may act as large antennae picking up noise and are susceptible to lightning strikes. Monitoring a large structure requires a network of a large number of rather expensive sensors that cannot be multiplexed, and each of them requires cumbersome and labor-intensive installation of long, heavy, and expensive electrical cables in need of extensive shielding and waterproofing. This PI has instrumented three highway bridges and one building with permanently installed sensors and experienced the difficulties associated with the conventional sensors. Emerging optical fiber sensing technologies can alleviate these difficulties, but very few optical fiber sensors, particularly dynamic sensors (such as accelerometers), have been successfully commercialized for bridge applications due to issues with reliability, field ruggedness, or cost issues.

With the unique sensing mechanism and the associated technical/cost advantages, the optical fiber dynamic sensor developed in this IDEA project has a great potential to be widely deployed in the field to monitor dynamic response of bridges for long-term structural health monitoring. The real-time information can be used not only for assessing post-event bridge damage and capacity for effective emergency response, but also for prioritizing structural rehabilitation and maintenance, as well as improvement of bridge structural design.